

16 **ABSTRACT**

17 Human astrovirus nonstructural protein nsP1a/4, located at the C-terminal end of
18 nsP1a, is thought to be involved in the regulation of RNA replication and capsid
19 maturation; however, its roles in viral growth and virulence are not well understood.
20 We investigated the intracellular host proteins that interact with nsP1a and
21 explored the potential roles of the interaction in the pathogenesis of human
22 astrovirus infection. We screened 14 independent proteins with a cDNA library
23 derived from Caco-2 cells using a yeast two-hybrid technique. Deletion analysis
24 revealed that interaction between the nsP1a/4 domain and the large extracellular
25 loop (LEL) domain of the human protein CD63 is necessary for astrovirus
26 replication. The interaction was confirmed by glutathione-S-transferase (GST)
27 pull-down assays and co-immunoprecipitation assays. Confocal microscopy
28 showed that nsP1a/4 and CD63 co-localized in the cytoplasm of infected cells.
29 Over expression of CD63 promoted viral RNA synthesis, whereas knockdown
30 of CD63 markedly decreased viral RNA levels. Those results suggest that CD63
31 plays a critical role in human astrovirus RNA replication. The interaction
32 between CD63 and nsP1a/4 provides a channel to further understand the roles of
33 interactions between host and virus proteins in astrovirus infection and release.

34

35 **IMPORTANCE**

36 Human astroviruses cause gastroenteritis in young children and
37 immunocompromised patients. In this study, we provide evidence that nsP1a/4,

38 a nonstructural protein located at the C-terminal end of the human astrovirus
39 nsP1a polyprotein, interacts with the host protein CD63. Over expression of
40 CD63 promoted viral RNA replication, whereas knockdown of CD63 decreased
41 virus RNA replication, indicating that CD63 plays a critical role in the human
42 astrovirus life cycle.

43

44 **KEYWORDS:** human astrovirus, HAstV, protein-protein interaction, nsP1a,
45 nsP1a/4, CD63, virus replication

46

47 Viruses are obligate intracellular pathogens that utilize host-cell machinery to
48 infect cells, replicate themselves, and then exit the cells for another round of
49 infection. Human astroviruses (HAstVs) are a group of non-enveloped,
50 single-stranded, and positive-sense RNA viruses in the family *Astroviridae*.
51 HAstVs are causative agents of viral diarrhea in young children,
52 immunocompromised patients, and elderly individuals (1-5). The astrovirus
53 genome has three open reading frames (ORFs); ORF1a and ORF1b encode two
54 nonstructural polyproteins (nsPs), and ORF2 encodes the capsid protein (6). The
55 nsP1a polyprotein, transcribed from ORF1a, is involved in viral transcription
56 and replication. When HAstV infects a host cell, nsP1a is cleaved into at least
57 four products, named nsP1a/1, nsP1a/2, nsP1a/3 (protease), and nsP1a/4. The
58 nsP1a/4 protein is located at the C-terminal end of nsP1a. Several domains have
59 been identified in nsP1a/4, including two coiled-coil regions, a death domain
60 (DD), a nuclear localization signal (NLS), a putative viral genome-linked
61 protein (VPg), and a hypervariable region (HVR) (7-12). It was confirmed that
62 nsP1a/4 plays important roles in the activation of capsid maturation and the
63 regulation of RNA replication (13, 14). To better understand the roles of nsP1a
64 and nsP1a/4 in HAstV infection and replication, we characterized host proteins
65 that interact with nsP1a or nsP1a/4 by utilizing a yeast two-hybrid approach. We
66 identified at least 14 host proteins that could bind to nsP1a, one of which was
67 CD63.

68 CD63, a member of the tetraspan transmembrane protein family, is a

69 four-span membrane protein that is widely distributed in multicellular organisms
70 and known to be associated with virus functions, such as adhesion, fusion, and
71 trafficking (15, 16). Tetraspanins, a large superfamily of cell-surface membrane
72 proteins characterized by four transmembrane domains, have the unique
73 property to form a network of protein-protein interactions through associations
74 with multiple membrane proteins that are involved in several infectious diseases
75 (17, 18). There is increasing evidence suggesting that intracellular pathogens,
76 especially viruses, “hijack” tetraspanins when entering, traversing and exiting
77 cells during the course of infection. Several studies have reported that
78 tetraspanins, such as CD151 (19), CD81 (20, 21), CD82 (22), CD9 (23), and
79 CD63 (24), are key players in the lifecycles of many viruses.

80 In this study, we used co-immunoprecipitation and
81 glutathione-S-transferase(GST) pull-down assays to confirm that CD63 can
82 interact with nsP1a/4. Confocal microscopy revealed that the CD63 large
83 extracellular loop (LEL) domain co-localizes with nsP1a/4 in the cytoplasm.
84 CD63 knockdown or overexpression strongly affected the replication of HAstV
85 in Caco-2 cells. Those findings indicate that CD63 plays an important role in the
86 HAstV life cycle.

87

88 **RESULTS**

89 **A yeast two-hybrid screen with nsP1a and a Caco-2 cDNA library**
90 **identified CD63 as a host protein that interacts with nsP1a.** We investigated

91 the interactions between HAstV nsP1a and host proteins using a protein-protein
92 overlay assay. We amplified the nsP1a gene by PCR and inserted the resulting
93 PCR product (2781bp) by recombination cloning into the yeast two-hybrid
94 (Y2H) bait vector pGBKT7 as a C-terminal fusion with a Gal4 DNA-binding
95 domain (BD). We confirmed the correct constructs by enzyme digestion and
96 DNA sequence analysis (Fig 1A). When introduced alone into yeast Y2HGold
97 cells, the Gal4 (BD)-nsP1a bait construct was not toxic to the yeast and did not
98 auto-activate the Y2H reporter gene, indicating that the construct was suitable
99 for use in a Y2H screen (Fig 1B).

100 Using a Y2H assay with Gal4 (BD)-nsP1a as bait and a human Caco-2 cDNA
101 prey library, we screened approximately 2.5×10^5 clones and identified 14
102 positive bait-prey interactions. Sequence and bioinformatics analysis of the 14
103 positive prey plasmids, listed by their initial positive-interaction identification
104 number, indicated that they represented 14 different human cDNAs (data not
105 shown). We next measured the strength of interaction between the nsP1a bait and
106 each of the 14 human prey proteins in yeast using a qualitative growth assay and
107 quantitative β -galactosidase activity assays. We performed bioinformatic
108 analysis of the human proteins confirmed by the qualitative growth assay to gain
109 functional insights into the potential interactions between those proteins and
110 nsP1a (Fig 2). We selected one host protein, identified as tetraspan
111 transmembrane protein CD63 (GenBank accession number: NM_001040034.1),
112 for further study.

113 **nsP1a interacts with CD63 *in vivo*.** We transfected HEK293 T cells with
114 PEF-HA-nsP1a and pcDNA3.1-3flag-CD63. After 48 h, we performed
115 immunoprecipitation with the cell lysates from those cells using an anti-Flag M2
116 Affinity Gel (Sigma, St. Louis, MO, USA). We analyzed the resulting protein
117 complexes by western blot with anti-Flag or anti-HA antibody (Fig. 3A). We
118 detected no proteins in control lysates from cells transfected with empty vector
119 (Fig. 3A, lane 1). We detected CD63 protein only in the lysates from cells that
120 were transfected with pcDNA3.1-3flag-CD63 (Fig. 3A, lane 2). Likewise, we
121 detected nsP1a protein only in the lysates from cells that were transfected with
122 PEF-HA-nsP1a (Fig. 3A, lane 3). Both nsP1a and CD63 were readily detected in
123 the lysates from cells that were co-transfected with pcDNA3.1-3flag-CD63 and
124 PEF-HA-nsP1a. The HA antibody was able to pull down CD63-Flag together
125 with nsP1a-HA (Fig. 3A, lane 4). Likewise, the Flag antibody was able to pull
126 down nsP1a-HA together with CD63-Flag (Fig. 3A, lane 4). Taken together, the
127 results suggested that nsP1a was able to interact with the CD63 *in vivo*.

128 **nsP1a interacts with CD63 *in vitro*.** To further investigate the interaction
129 between nsP1a and CD63, we determined whether the interaction occurs
130 *in vitro*. We expressed recombinant full-length nsP1a-GST fusion protein
131 (≈ 118 kDa) induced by isopropyl β -D-thiogalactopyranoside (IPTG) in
132 *Escherichia coli* (Fig. 3B lanes 1–6). We also detected purified nsP1a from the
133 bacteria (Fig. 3B lane 7) and human CD63 His Tag commercialized recombinant
134 protein (≈ 26 kDa) by western blot (Fig. 3B lane 8). We tested the interaction

135 between CD63 and nsP1a by GSTpull-down analysis. We immobilized
136 nsP1a-GST on glutathione agarose and added CD63-His to assess
137 protein-protein binding. We used an untreated gel as a negative control. We
138 analyzed the protein in the complexes by western blot with anti-GST or anti-His
139 antibody. Anti-GST MAb pulled down nsP1a together with CD63 (Fig. 3C).
140 Consistent with those results, anti-His MAb could pull down CD63 protein
141 together with nsP1a protein. In contrast, the negative control could not pull
142 down any viral proteins. The results indicated that nsP1a could interact with
143 CD63 *in vitro*.

144 **The nsP1a/4 protein interacts with the CD63 large-loop domain.** We
145 performed binding experiments to identify the region of the nsP1a protein that
146 interacts with CD63 *in vivo* and *in vitro*. CD63 contains 204–355 amino acids
147 (20–30 kDa), comprising four transmembrane domains, a short extracellular
148 loop (EC1), a long extracellular loop (EC2), a very short intracellular loop, and
149 cytoplasmic N-terminal and C-terminal tails (Figure 4A). EC2, also called the
150 large loop (LEL, 99aa), contains a variable region for specific protein-protein
151 interactions. We constructed and confirmed the eukaryotic expression vector
152 pcDNA3.1-3flag-CD63-LEL and the prokaryotic expression vector
153 pET-29a-LEL. We expressed IPTG-induced recombinant CD63-LEL-His fusion
154 protein in *E. coli* and recovered and purified the recombinant protein from the
155 bacteria (Fig 4C).

156 We amplified the four products of the nsP1a polyprotein (nsP1a/1, nsP1a/2,

157 nsP1a/3 (protease), and nsP1a/4; Fig 4B) by RT-PCR. We used the PCR
158 products to construct PEF-HA-1a/1, PEF-HA-1a/2, PEF-HA-1a/3, and HA-1a/4
159 plasmids, which we confirmed by sequencing. We expressed recombinant
160 nsP1a/4-GST fusion protein in bacteria and isolated and purified the fusion
161 protein from the bacteria (Fig4D). We co-transfected HEK293T cells with
162 pcDNA3.1-3flag-CD63-LEL and either PEF-HA-1a/1, PEF-HA-1a/2,
163 PEF-HA-1a/3, or PEF-HA-1a/4. We then performed immunoprecipitation with
164 lysates from the transfected cells and anti-HA or anti-Flag antibodies. We
165 identified protein-protein interactions by GST pull-down (Fig 4E) or
166 co-immunoprecipitation (Fig 4F) assays as described above. The results showed
167 that the CD63 LEL domain interacted with nsP1a/4 *in vivo* and *in vitro*. In
168 contrast, no interaction between CD63-LEL and nsP1a/1, nsP1a/2, or nsP1a/3
169 were observed (data not shown).

170 **CD63-LEL co-localizes with nsP1a/4 in host cells.** We used
171 immunofluorescence and confocal microscopy to further investigate the
172 interaction between nsP1a/4 and CD63-LEL. We co-transfected HEK293T cells
173 with the plasmids HA-nsP1a/4 and Flag-CD63-LEL. We then examined the
174 subcellular localization of nsP1a/4 and CD63-LEL by confocal microscopy. The
175 Flag-CD63-LEL (Fig. 5A) and HA-nsP1a/4 (Fig. 5B) proteins were distributed
176 throughout the cytoplasm. We determined the position of the nucleus by DAPI
177 staining (Fig. 5C). Statistical analysis of the images showed that the
178 (immunofluorescence assay, IFA) signals of nsP1a/4 and CD63-LEL significantly

179 overlapped each other (Fig 5D). That finding confirmed that nsP1a/4 protein
180 interacts with CD63-LEL in HEK293T cells. That result along with those of a
181 previous Y2H screen and GSTpull-down and co-immunoprecipitation assays
182 suggested that nsP1a/4 interacts with the CD63LEL domain.

183 **HAsV infection increases CD63 expression.** HAsV-1 nsP1a has been
184 reported to regulate the viral RNA-replication process. To determine whether
185 HAsV-1 infection affects CD63 expression, we infected Caco-2 cells with
186 HAsV-1 (MOI 10). We collected lysates from mock-infected (control) and
187 HAsV-infected cells 24h and 48h after infection. We isolated total cellular RNA
188 and quantified the expression of CD63 mRNA using real-time RT-PCR(Fig. 6A).
189 We also performed western blot to detect CD63 protein expression in the
190 cellular lysates (Fig 6B). The results showed that the levels of CD63 mRNA and
191 protein 48h after infection were higher in HAsV-infected cells than
192 in mock-infected cells, suggesting that CD63 plays an important role in HAsV-1
193 genome replication. Furthermore, we infected Caco-2 cells with HAsV-1(MOI
194 1) and measured the amount of viral RNA present in the cell culture after 24h
195 and 48h. The results showed that the amount of viral RNA was significantly
196 increased at 24h and 48h in the HAsV-1-infected cells compared with those in
197 the mock-infected cells ($P < 0.01$; Fig 6C).

198 **CD63 expression affects HAsV replication.** To assess the role of CD63 in
199 HAsV replication, we infected CD63-overexpressing and CD63-knockdown
200 Caco-2 cells with HAsV-1 and measured the level of viral RNA 48 h after

201 infection. We assessed the overexpression and knockdown of CD63 by western
202 blot and real-time RT-PCR, respectively (Fig. 6D and E). CD63 expression
203 relative to the wild-type level was increased 5-fold in the cells transfected with
204 the overexpression plasmid and decreased 10-fold in the cells transfected with
205 the anti-CD63 shRNA. We then infected the cells with HAstV-1 (MOI 1) and
206 measured the amount of viral RNA present in the cell cultures 48h after
207 infection. The results showed a 1.45-fold increase in the level of HAstV-1 RNA
208 in the cultures of CD63-overexpressing cells compared with that in cultures of
209 control cells ($P < 0.01$). The CD63 knockdown resulted in a 6-fold decrease
210 in intracellular viral RNA levels ($P < 0.01$; Fig 6F). Those results indicated that
211 CD63 plays an important role in the HAstV lifecycle.

212

213 **DISCUSSION**

214 Positive-sense RNA viruses have frequently been found to replicate in
215 association with a large number of cellular proteins (25). The C-terminal nsP1a
216 protein of HAstV Yuc8 was shown to interact with the viral polymerase (14).
217 Astrovirus replication and assembly have also been linked to fatty-acid synthesis,
218 ATP biosynthesis, and cellular lipid metabolism (26), but it is unknown what
219 host proteins contribute to a successful virus infection. We found that HAstV
220 nsP1a or nsP1a/4 could interact with the host protein CD63 based on a Y2H
221 screen and observations of direct interaction between nsP1a/4 and CD63 both
222 *in vivo* and *in vitro*.

223 Although the function of HAstVnsP1a remains unclear, nsP1a and nsP1a/4
224 have been suggested to be involved in many processes, including genome
225 replication, apoptosis induction, and capsid maturation (8, 11). To better
226 understand the role of nsP1a in viral replication, we analyzed the interaction of
227 nsP1a with host proteins. A Y2H screen of aCaco-2 cDNA library showed that
228 14 independent proteins, including CD63, interacted with nsP1a.

229 CD63 was the first characterized tetraspanin(27). It has been shown that
230 CD63 reacts with many different proteins either directly or indirectly, including
231 integrins(28,29), other tetraspanins(30,31), cell-surface receptors(32), and
232 kinases(33). Viruses are obligate intracellular pathogens and must utilize
233 host-cell machinery in order to complete their lifecycle. Viruses have been
234 shown to incorporate many host components, including tetraspan
235 transmembrane proteins (34). It is therefore highly likely that tetraspanins play
236 an important role in the lifecycles of viruses. We confirmed that CD63 could
237 interact with HAstV nsP1a both *in vivo* and *in vitro*. We transfected HEK293T
238 cells with nsP1a-HA alone or together with CD63-Flag. We successfully
239 recovered nsP1a-HA/CD63-Flag complex by co-immunoprecipitation assays of
240 co-transfected cells. We showed that CD63 bound directly to nsP1a *in vitro*
241 using GST pull-down analyses of purified recombinant GST-nsP1a protein and
242 recombinant CD63-His protein. Those results showed that the HAstV nsP1a
243 could interact with CD63.

244 In light of those results, we sought to explore the nsP1a/CD63 interaction in

245 more detail. GSTpull-down and co-immunoprecipitation analyses showed that
246 the nsP1a C-terminal nonstructural protein nsP1a/4 (567–926aa, 40kDa) binds to
247 the CD63 LEL domain. The LEL of CD63 displays some conserved residues.
248 Protein-protein interaction sites have been found in the LEL domains of other
249 proteins (35, 36). We verified that the CD63-LEL domain interacts with nsP1a/4
250 *in vivo* and *in vitro*. Confocal microscopy also showed that nsP1a/4 and CD63
251 co-localized in the cytoplasm. Previous data indicated that the HAstV nsP1a
252 polyprotein would generate at least four products. The nonstructural C-terminal
253 protein of nsP1a, which contains a hypervariable region, has been named nsP1a/4.
254 The nonstructural N-terminal protein including nsP1a/1, nsP1a/2, and nsP1a/3 of
255 the nsP1a polyprotein cannot interact with CD63, suggesting that nsP1a interacts
256 with CD63 through its C-terminal region.

257 Tetraspanin proteins have been reported to be involved in the lifecycles of
258 many viruses, such as human immunodeficiency virus (HIV)(37-39), hepatitis C
259 virus (HCV) (40,41), human papillomavirus(HPV) (42,43), human T cell
260 lymphotropic virus (HTLV) (44), porcine reproductive and respiratory
261 syndrome virus (PPRSV) (45), and rotavirus(46). CD63 protein was confirmed
262 to interact with the rotavirus VP6 protein and to be involved in the release of
263 membrane vesicles by intestinal epithelial cells infected with rotavirus (47).
264 CD63 also has been shown to play an essential role during HIV-1 replication in
265 macrophages. CD63 can interact with and accumulate in close proximity to the
266 HIV gp41 protein during the cell-to-cell transfer of HIV (48).

267 We constructed CD63-knockdown and CD63-overexpressing cells lines to
268 determine if CD63 expression affects HAstV-1 replication. CD63 overexpression
269 increased the viral mRNA level in infected cells, whereas CD63 knockdown
270 reduced the viral mRNA level in infected cells. A previous study suggested
271 that nsP1a/4 is involved in the viral RNA replication process and might be
272 necessary for efficient formation of the viral RNA-replication complex through
273 a direct interaction with the viral RNA or with other proteins of the complex
274 (14). Further research is needed to investigate whether CD63 or nsP1a/4 is
275 necessary for viral RNA or viral polymerase to form a functional replication
276 complex and to identify which signal pathway is involved promoting virus
277 replication.

278 We confirmed that CD63 is co-opted by HAstV nsP1a/4 during infection of
279 susceptible host cells. The interaction between CD63 and nsP1a/4 appears to
280 promote viral RNA replication. Our results confirmed that CD63 is involved in
281 the formation of exosomes and is abundantly present in late endosomes and
282 lysosomes. CD63 at the cell surface is endocytosed via a clathrin-dependent
283 pathway. In late endosomes, CD63 is enriched on the intraluminal vesicles,
284 which are secreted by specialized cells as exosomes via the fusion of endosomes
285 with the plasma membrane. HAstV Yuc8 RNA replication occurs in association
286 with host-cell membranes, and the entry of HAstV into host cells apparently
287 depends on the maturation of endosomes (49). The significance of CD63
288 function in HAstV infection and whether CD63 is involved in HAstV cell

289 binding, endocytosis, membrane vesicles, post-entry processing, or virus
290 maturation still remains to be determined. We hypothesize that the CD63/nsP1a
291 interaction plays a role in viral RNA replication, and further study is needed to
292 verify that hypothesis.

293

294 **MATERIALS AND METHODS**

295 **Cell culture and virus infection.** HEK293T and Caco-2 cells were
296 maintained in Dulbecco's Modified Eagle's Medium (DMEM; GIBCO, UK)
297 containing 10% fetal calf serum (GIBCO, UK). A plasmid-based reverse
298 genetics system for human astrovirus type 1 (HAstV-1) was provided by
299 professor Akira Nakanishi, Department of Aging Intervention, National Center
300 for Geriatrics and Gerontology Morioka, Obu, Aichi, Japan. An HAstV-1cDNA
301 plasmid (pCAG-AVIC) that drives HAstV-1 cDNA expression from the CAG
302 promoter was transfected into HEK293T cells. Cell-culture supernatants were
303 collected 48 h after transfection and used as a source of recombinant viruses to
304 infect Caco-2 cells (50). The virus was activated with 200 µg/mL porcine
305 trypsin(Sigma) for 1h at 37°C before exposure to the cells. The virus titers in the
306 Caco-2 cell cultures were determined by fluorescent-focus assays as described
307 previously (50).

308 **Construction and expression of plasmids.** HAstV-1 nsP1a protein
309 (GenBank accession number: AGX15183.1) was amplified using primers listed
310 in Table 1 and cloned into pGBKT7 vector (Clontech USA, Mountain View, CA)

311 to generate BD-bait plasmid (pGBKT7-nsP1a) for the Y2H system. To generate
312 N-terminally HA-tagged nsP1a and nsP1a/4 expression constructs, nsP1a or
313 nsP1a/4 frames were amplified using the primers listed in Table 1. We extracted
314 the total RNA of HAstV type 1 (HAstV-1) from Caco-2 cells and amplified
315 nsP1a by RT-PCR. The PCR products were cloned into PEF-HA PGK Hygrp
316 vector to create PEF-HA-nsP1a and PEF-HA-nsP1a/4 plasmids via the in-fusion
317 HD Cloning method (TaKaRa Bio, Dalian, China). The expression plasmids
318 pGEX-6P-1-nsP1a and pGEX-6P-1-nsP1a/4 were generated via the insertion of
319 nsP1a or nsP1a/4 cDNA between the *Bam*H I and *Xho* I sites of pGEX-6P-1.
320 The expression plasmid pET-29a-CD63-LEL was generated via the insertion
321 of CD63-LEL cDNA between the *Xho* I and *Bam*H I sites of pET-29. To generate
322 N-terminally Flag-tagged CD63 (GenBank accession number: NM_001040034.1)
323 or CD63-LEL expression constructs, CD63 or CD63-LEL PCR products were
324 cloned into pcDNA3.1(+) vector to create pcDNA3.1-3flag-CD63 and
325 pcDNA3.1-3flag-CD63-LEL via the in-fusion HD Cloning method.

326 **Expression and purification of recombinant nsP1a, nsP1a/4, and LEL**
327 **proteins.** The nsP1a and nsP1a/4 proteins were expressed and purified using
328 the same protocol was used for the CD63-LEL protein with some modifications.
329 Briefly, the recombinant plasmid was transformed into competent *E. coli* BL21
330 (DE3) cells, which were then grown overnight in 5 mL Luria-Bertani broth. The
331 incubation was continued until the optical density (OD₆₀₀) reached 0.6–0.8.
332 The expression of the protein was induced with 0.1–1 mM IPTG at 25–37°C

333 withshaking at 220 rpm. Expression of the protein was then analyzed by
334 SDS-PAGE. Supernatant containing the fusion protein was purified using
335 Glutahione Sepharose 4B (GE Healthcare Bio-Sciences, Little Chalfont, UK)
336 according to the manufacturer's instructions. The purification of recombinant
337 nsP1a, nsP1a/4, and LEL proteins was further confirmed by western blot.

338 **Plasmid transfection.** HEK293T cells were transfected with plasmids
339 containing recombinant DNA using the Lipofectamine 2000 transfection reagent
340 (Invitrogen) according to the manufacturer's protocol. Briefly, cells were grown
341 to approximately 90% confluence on six-well palates. The culture medium was
342 replaced by serum-free medium containing the desired plasmid and
343 Lipofectamine2000. The cells were incubated for 48 h at 37°C in 5% CO₂ and
344 harvested for examination by western blot analysis to confirm the protein
345 expression.

346 **Antibodies.** Anti-Flag murine IgG1 monoclonal antibody, anti-HA murine
347 IgG1 monoclonal antibody, rabbit antibody, anti-GST-Tag mouse polyclonal
348 antibody, and anti-His-tag mouse polyclonal antibody were used (Sigma).
349 Horseradish peroxidase-labeled goat anti-mouse IgG or goat anti-rabbit IgG
350 (Santa Cruz Biotechnology Co.,Ltd, Shanghai, China) were used for western
351 blotting. FITC-labeled goat anti-mouse IgG and Alexa Fluor®-labeled Goat
352 Anti-rabbit IgG (Santa Cruz Biotechnology) were used as secondary antibodies
353 for immunofluorescence and confocal microscopy. A polyclonal antibody to
354 recombinant nsP1a or nsP1a/4 of HAstV was prepared in a previous study (51).

355 **Isolation of nsP1a-interacting cDNA clones using the Y2H technique.**

356 A full-length expression cDNA library derived from the Caco-2 cell line was
357 constructed for three ORFs. Y2H media set (Clontech, TaKaRa Biomedical
358 Technology Co., Ltd., Dalian, China) was used to identify nsP1a binding factors
359 according to the manufacturer's instructions. In brief, AH109 and Y187 cells
360 were transformed with the bait (pGBKT7-nsP1a) and prey (Caco-2 cDNA
361 library) constructs, respectively, according to the yeast transformation protocol
362 (Clontech). A clone of the bait transformant was mated with a clone of the prey
363 transformant and grown at 30°C overnight in 1 mL yeast extract peptone
364 dextrose broth. The mated clones were selected on SD medium fortified with
365 tryptophan and leucine to ensure successful mating. Finally, the interacting
366 partners were screened on SD media lacking tryptophan (-Trp), leucine (-Leu),
367 adenine (-Ade), and histidine (-His). Plasmids pGBKT7-53 and pGADT7-T,
368 encoding the interacting protein pair P53 and Simian virus 40 (SV40) large T
369 antigen, respectively, were used as positive controls. Plasmids pGBKT7-Lam
370 and pGADT7-T, encoding the non-interacting protein pair lamin and SV40 large
371 T antigen, respectively, served as negative controls.

372 **Western blot.** Protein samples were separated by 12% SDS-PAGE and then
373 transferred onto PVDF membranes (Millipore, Bedford, MA, USA). The
374 membranes were incubated with anti-HA mAb(1:5000), anti-Flag
375 mAb(1:10000), anti-CD63 mAb (1:2000), and anti-CD63 mAb
376 (1:1000), respectively. The membranes were subsequently rinsed with PBST and

377 treated with HRP-labeled goat anti-mouse IgG or goat anti-rabbit IgG as the
378 secondary antibody (1:3000) (Santa Cruz Biotechnology). The proteins were
379 visualized via scanning with ECL prime western blotting detection reagent
380 (Beyotime Biotechnology, Beijing, China).

381 **GST pull-down assays.** The recombinant pGEX-6P-1-nsP1a or
382 pGEX-6P-1-nsP1a/4 plasmids were used to transform competent *E. coli* BL21
383 (DE3) cells. The cells were then grown overnight in 5 mL Luria-Bertani broth
384 supplemented with ampicillin until the optical density (OD₆₀₀) reached 0.6–0.8.
385 Expression of pGEX-6P-nsP1a was induced with 0.1~1 mM IPTG at 25~37°C
386 with shaking at 220 rpm and then analyzed by SDS-PAGE. GST-nsP1a protein
387 was purified using a gravity-flow GST-Sefinose™ Resin (Sangon Bitech,
388 Shanghai, China) column according to the manufacturer's instructions and
389 detected by SDS-PAGE. His-tagged recombinant human CD63 protein was
390 obtained from ThermoFisher Scientific Sino Biological (China). The expression
391 and purification of the CD63 LEL domain were performed by the same method
392 used for nsP1a and nsP1a/4. The Pierce™ GST Protein Interaction Pull-Down
393 Kit (Thermo Fisher Scientific) was used to identify the interaction between
394 nsP1a or nsP1a/4 and CD63 or CD63-LEL *in vitro*. In brief, prepared
395 GST-nsP1a or GST-nsP1a/4 bait protein sample was bound to glutathione
396 agarose. Then, the beads were washed four times with wash solution
397 (25 mM Tris-HCl, 0.15 M NaCl, pH 7.2). Pull-Down Lysis Buffer was incubated
398 with recombinant His-tagged CD63 or His-CD63-LEL at 4°C for at least 1 h

399 with gentle shaking. The eluted proteins were detected by SDS-PAGE followed
400 by western blot analysis with anti-GST antibody and CD63 antibody.

401 **Co-immunoprecipitation of nsP1a/4 with CD63-LEL.** HEK293T cells
402 were transfected with PEF-HA-nsP1a/4 and pcDNA3.1-3flag-CD63-LEL
403 expression plasmids. Following transfection for 48 h, the cells were lysed in
404 NP-40 lysis buffer containing protease inhibitors. Following the manufacturer's
405 protocol, antibodies directed against Flag or HA were separately bound and
406 cross-linked to Protein G Dynabeads (Novagen) using the reagents provided in
407 the Pierce Crosslink Co-immunoprecipitation Kit (Pierce). Approximately 1–5
408 mg of untransfected or transfected cell lysates were then mixed with different
409 sets of antibody-coupled beads and washed. The eluted proteins were analyzed
410 by western blot using Flag or HA antibody.

411 **Immunofluorescence and confocal microscopy.** HEK293T cells were
412 co-transfected with PEF-HA-nsP1a/4 and pcDNA3.1-3flag-CD63-LEL plasmids.
413 After 48 h, the cells were washed with 1 mL PBS and fixed with 4%
414 paraformaldehyde for 10min at room temperature. After additional PBS washes,
415 mouse anti-Flag and rabbit anti-HA was applied at a dilution of 1:1000. The cells
416 were then incubated for 1h at room temperature, washed with PBS, and
417 subsequently incubated with FITC-labeled goat anti-mouse IgG and Alexa
418 Fluor®-labeled goat anti-rabbit IgG at a dilution of 1:500. The cells were then
419 washed with PBS and observed under a confocal microscope.

420 **CD63 overexpression and knockdown.** The primers used to construct

421 pcDNA3.1-3flag-CD63 are listed in Table 1. Two pairs of shRNAs targeting
422 human CD63 and a negative control shRNA (Table 1) were cloned into
423 hU6-MCS-CMV-GFP-SV40-Neomycin vector (Shanghai Genechem Co.,Ltd.)
424 to generate CD63-shRNA-1, CD63-shRNA-2, and CD63-NC, respectively.
425 HEK293T cells were transfected with the constructs along with
426 pcDNA3.1-3flag-CD63 using Lipofectamine 2000 transfection reagent
427 (Invitrogen, Carlsbad, CA) following the manufacturer's protocol.

428 **Real-time RT-PCR.** The target gene CD63 and HAsV RNA were quantified
429 by real-time RT-PCR using the primers listed in Table 1. Total RNA was
430 isolated from HEK293T cells using TRIzol (Invitrogen) according to the
431 manufacturer's instructions. cDNA was reverse transcribed from 1 μ g total RNA
432 using PrimeScript Reverse Transcriptase (TaKaRa Bio,Dalian,China).
433 Quantitative real-time RT-PCR was performed using the SYBR PrimeScript
434 RT-kit(TaKaRa Bio) according to the manufacturer's instructions. The relative
435 transcript levels were analyzed using the $\Delta\Delta$ Ct method. The results were
436 analyzed using Bio-RAD IQTM5 optical system software.

437 **Statistical analysis.** Data were presented as the mean \pm SD. Differences
438 between groups were examined using Student's t test with $P < 0.05$ as the
439 threshold for statistical significance.

440

441 **ACKNOWLEDGMENTS**

442 This work was supported by grants from the National Nature Science

443 Foundation of China (no. 81201285), the National Nature Science Foundation of
444 Liaoning Province (no.20170540398), and the Biological Anthropology
445 Innovation Team Project of JZMU (no.JYLJ201702)

446

447

448

449 REFERENCES

450 1. Méndez EA, Arias CF. 2013. Astroviruses, p 609–628. In Knipe DM,Howley PM, Cohen
451 JI, Griffin DE, Lamb RA, Martin MA, Racaniello VR,Roizman B (ed), Fields virology,
452 6th ed, vol 1. Lippincott Williams &Wilkins, Philadelphia, PA.

453 2. Gallimore CI, Taylor C, Gennery AR, Cant AJ, Galloway A, Lewis D,Gray JJ. 2005. Use
454 of a heminested reverse transcriptase PCR assay for detection of astrovirus in
455 environmental swabs from an outbreak of gastroenteritis in a pediatric primary
456 immunodeficiency unit. *J Clin Microbiol* 43(8):3890–3894.

457 3. Wunderli W, Meerbach A, Güngör T, Berger C, Greiner O, Caduff R, Trkola A, Bossart W,
458 Gerlach D, Schibler M, Cordey S, McKee TA, Van Belle S, Kaiser L, Tapparel C.2011.
459 Astrovirus infection in hospitalized infants with severe combined immunodeficiency after
460 allogeneic hematopoietic stem cell transplantation. *PLoS One* 6(11):e27483.

461 4. Silva RC, Benati FJ, Pena GP, Santos N.2010. Molecular characterization of viruses
462 associated with gastrointestinal infection in HIV-positive patients. *Braz J Infect Dis*
463 14(6):549-552.

464 5. Quan PL, Wagner TA, Briese T, Torgerson TR, Hornig M, Tashmukhamedova A, Firth C,

- 465 Palacios G, Baisre-De-Leon A, Paddock CD, Hutchison SK, Egholm M, Zaki SR,
466 Goldman JE, Ochs HD, Lipkin WI. 2010. Astrovirus encephalitis in boy with X-linked
467 agammaglobulinemia. *Emerg Infect Dis.* 16(6):918-925.
- 468 6. De Benedictis P, Schultz-Cherry S, Burnham A, Cattoli G. 2011. Astrovirus infections in
469 humans and animals - Molecular biology, genetic diversity, and interspecies
470 transmissions. *Infect Genet Evol* 11(7):1529-1544.
- 471 7. Al-Mutairy B, Walter JE, Pothen A, Mitchell DK. 2005. Genome prediction of putative
472 genome-linked viral protein (VPg) of astroviruses. *Virus Genes* 31(1):21–30.
- 473 8. Guix S, Bosch A, Ribes E, Dora Martínez L, Pintó RM. 2004. Apoptosis in
474 astrovirus-infected CaCo-2 cells. *Virology* 319(2):249–261.
- 475 9. Jiang B, Monroe SS, Koonin EV, Stine SE, Glass RI. 1993. RNA sequence of astrovirus:
476 distinctive genomic organization and a putative retrovirus-like ribosomal frameshifting
477 signal that directs the viral replicase synthesis. *Proc Natl Acad Sci U S A.*
478 90(22):10539–10543.
- 479 10. Méndez-Toss M, Romero-Guido P, Munguía ME, Méndez E, Arias CF. 2000. Molecular
480 analysis of a serotype 8 human astrovirus genome *J Gen Virol* 81(Pt 12):2891–2897.
- 481 11. Willcocks MM, Boxall AS, Carter MJ. 1999. Processing and intracellular location of
482 human astrovirus non-structural proteins. *J Gen Virol* 80(Pt 10):2607–2611.
- 483 12. Méndez E, Salas-Ocampo MP, Munguía ME, Arias CF. 2003. Protein products of the
484 open reading frames encoding nonstructural proteins of human astrovirus serotype 8. *J*
485 *Virol* 77(21):11378–11384.
- 486 13. Guix S, Caballero S, Bosch A, Pintó RM. 2005. Human astrovirus C-terminal nsP1a

- 487 protein is involved in RNA replication. *Virology* 333(1), 124-31.
- 488 14. Fuentes C, Guix S, Bosch A, Pintó RM. 2011. The C-terminal nsP1a protein of human
489 astrovirus is a phosphoprotein that interacts with the viral polymerase. *J Virol*
490 85(9):4470-4479.
- 491 15. Pals MS, Klumperman J. 2009. Trafficking and function of the tetraspanin CD63. *Exp*
492 *Cell Res* 315(9):1584-1592.
- 493 16. Hassuna N, Monk PN, Moseley GW, Partridge LJ. 2009, Strategies for targeting
494 tetraspanin proteins: potential therapeutic applications in microbial infections. *BioDrugs*
495 23(6):341-359
- 496 17. Van Spriël AB, Figdor CG. 2010. The role of tetraspanins in the pathogenesis of
497 infectious diseases. *Microbes Infect* 12(2), 106-112.
- 498 18. Monk PN, Partridge LJ. 2012. Tetraspanins: gateways for infection. *Infect Disord Drug*
499 *Targets* 12(1), 4-17.
- 500 19. Hochdorfer D, Florin L, Sinzger C, Lieber D. 2016. Tetraspanin CD151 Promotes Initial
501 Events in Human Cytomegalovirus Infection. *J Virol* 90(14):6430-6442.
- 502 20. Fast LA, Lieber D, Lang T, Florin L. 2017. Tetraspanins in infections by human
503 cytomegalo- and papillomaviruses. *Biochem Soc Trans* 45(2):489-497.
- 504 21. Rocha-Perugini V, Suárez H, Álvarez S, López-Martín S, Lenzi GM, Vences-Catalán F,
505 Levy S, Kim B, Muñoz-Fernández MA, Sánchez-Madrid F, Yáñez-Mó M. 2017. CD81
506 association with SAMHD1 enhances HIV-1 reverse transcription by increasing dNTP
507 levels. *Nat Microbiol* 2(11):1513-1522.

- 508 22. Yu G, Bing Y, Li W, Xia L, Liu Z.2014. Hepatitis B virus inhibits the expression of
509 CD82 through hypermethylation of its promoter in hepatoma cells. *Mol Med Rep*
510 10(5):2580-2586.
- 511 23. Earnest JT, Hantak MP, Li K, McCray PB Jr, Perlman S, Gallagher T.2017. The
512 tetraspanin CD9 facilitates MERS-coronavirus entry by scaffolding host cell receptors
513 and proteases. *PLoS Pathogen* 13(7):e1006546.
- 514 24. Hurwitz SN, Nkosi D, Conlon MM, York SB, Liu X, Tremblay DC, Meckes DG Jr. 2017.
515 CD63 Regulates Epstein-Barr Virus LMP1 Exosomal Packaging, Enhancement of
516 Vesicle Production, and Noncanonical NF- κ B Signaling. *J Virol* 91(5). pii: e02251-16.
- 517 25. Ahlquist P, Noueir AO, Lee WM, Kushner DB, Dye BT. 2003. Host factors in
518 positive-strand RNA virus genome replication. *J Virol* 77(15):8181–8186.
- 519 26. Murillo A, Vera-Estrella R, Barkla BJ, Méndez E, Arias CF.2015. Identification of Host
520 Cell Factors Associated with Astrovirus Replication in Caco-2 Cells. *J Virol*
521 89(20):10359-10370.
- 522 27. Pols MS, Klumperman J. 2009.Trafficking and function of the tetraspanin CD63. *Exp*
523 *Cell Res* 315(9):1584-1592.
- 524 28. Berditchevski F.Complexes of tetraspanins with integrins: more than meets the eye.
525 2001. *J Cell Sci* 114(Pt 23):4143-4151.
- 526 29. Bassani S, Cingolani LA.2012. Tetraspanins: Interactions and interplay with integrins.
527 *Int J Biochem Cell Biol.* 44(5):703-708.
- 528 30. Radford KJ, Thorne RF, Hersey P.1996. CD63 associates with transmembrane 4
529 superfamily members, CD9 and CD81, and with beta 1 integrins in human melanoma,

- 530 Biochem. Biophys. Res. Commun 222(1):13-8
- 531 31. Berditchevski F, Odintsova E. 2007. Tetraspanins as regulators of protein trafficking.
532 Traffic.8(2):89-96
- 533 32. Yoshida T, Kawano Y, Sato K, Ando Y, Aoki J, Miura Y, Komano J, Tanaka
534 Y, Koyanagi Y. 2008. A CD63 mutant inhibits T-cell tropic human immunodeficiency
535 virus type 1 entry by disrupting CXCR4 trafficking to the plasma membrane. Traffic
536 9(4):540-558.
- 537 33. Latysheva N, Muratov G, Rajesh S, Padgett M, Hotchin NA, Overduin M, Berditchevski
538 F. 2006. Syntenin-1 is a new component of tetraspanin-enriched microdomains:
539 mechanisms and consequences of the interaction of syntenin-1 with CD63. Mol Cell Biol
540 26(20):7707-7718.
- 541 34. Monk PN, Partridge LJ. 2012. Tetraspanins: gateways for infection. Infect Disord Drug
542 Targets 12(1):4-17.
- 543 35. Stipp CS, Kolesnikova TV, Hemler ME. 2003. Functional domains in tetraspanin
544 proteins. Trends Biochem Sci 28(2):106-112.
- 545 36. Kitadokoro K, Bordo D, Galli G, Petracca R, Falugi F, Abrignani S, Grandi G, Bolognesi
546 M. 2001. CD81 extracellular domain 3D structure: insight into the tetraspanin
547 superfamily structural motifs. EMBO J 15; 20(1-2):12-8.
- 548 37. von Lindern JJ, Rojo D, Grovit-Ferbas K, Yeramian C, Deng C, Herbein G, Ferguson
549 MR, Pappas TC, Decker JM, Singh A, Collman RG, O'Brien WA. 2003.
550 Potential role for CD63 in CCR5-mediated human immunodeficiency virus type 1 infecti
551 on of macrophages. J Virol 77(6):3624-3633.

- 552 38. Li G, Dziuba N, Friedrich B, Murray JL, Ferguson MR.
553 A post-entry role for CD63 in early HIV-1 replication. *Virology* 412(2):315-324.
- 554 39. Chen H, Dziuba N, Friedrich B, von Lindern J, Murray JL, Rojo DR, Hodge TW, O'Brien
555 WA, Ferguson MR. 2008. A critical role for CD63 in HIV
556 replication and infection of macrophages and cell lines. *Virology* 379(2): 191-196.
- 557 40. Grigorov B, Molle J, Rubinstein E, Zoulim F, Bartosch B. 2017. CD81 large extracellular
558 loop-containing fusion proteins with a dominant negative effect on HCV cell spread and
559 replication. *J Gen Virol* 98(7):1646-1657.
- 560 41. Ramanathan A, Gusarova V, Stahl N, Gurnett-Bander A, Kyratsous CA. 2016.
561 Alirocumab, a Therapeutic Human Antibody to PCSK9, Does Not Affect CD81 Levels
562 or Hepatitis C Virus Entry and Replication into Hepatocytes. *PLoS One* 26;
563 11(4):e0154498.
- 564 42. Scheffer KD, Gawlitza A, Spoden GA, Zhang XA, Lambert C, Berditchevski F, Florin L.
565 2013. Tetraspanin CD151 mediates papillomavirus type 16 endocytosis. *J*
566 *Virology* 87(6):3435-3446.
- 567 43. Gräbel L, Fast LA, Scheffer KD, Boukhallouk F, Spoden GA, Tenzer S, Boller K, Bago
568 R, Rajesh S, Overduin M, Berditchevski F, Florin L. 2016.
569 The CD63-Syntenin-1 Complex Controls Post-Endocytic Trafficking of Oncogenic
570 Human Papillomaviruses. *Sci Rep* 6:32337.
- 571 44. Mazurov D, Heidecker G, Derse D. 2006. HTLV-1 Gag protein associates with
572 CD82 tetraspanin microdomains at the plasma membrane. *Virology* 346(1): 194-
573 204.

- 574 45. Shanmukhappa K, Kim JK, Kapil S.2007. Role of CD151, A tetraspanin, in porcine
575 reproductive and respiratory syndrome virus infection. *Virology* 16; 4:62.
- 576 46. Halasz P, Fleming FE, Coulson BS.2005. Evaluation of specificity and effects
577 of monoclonal antibodies submitted to the Eighth Human Leucocyte Differentiation
578 Antigen Workshop on rotavirus-cell attachment and entry. *Cell Immunology*
579 236(1-2):179-187.
- 580 47. Barreto A, Rodríguez LS, Rojas OL, Wolf M, Greenberg HB, Franco MA, Angel J.2010.
581 Membrane vesicles released by intestinal epithelial cells infected with
582 rotavirus inhibit T-cell function. *Viral Immunology* 23(6):595-608.
- 583 48. Ivanusic D.2014. HIV-1 cell-to-cell spread: CD63-gp41 interaction at
584 the virological synapse. *AIDS Research and Human Retroviruses* 30(9):844-845.
- 585 49. Méndez E, Muñoz-Yañez C, Sánchez-San Martín C, Aguirre-Crespo G, Baños-Lara
586 Mdel R, Gutierrez M, Espinosa R, Acevedo Y, Arias CF, López S.2014.
587 Characterization of human astrovirus cell entry. *Journal of Virology* 88(5):2452-2460.
- 588 50. Chapellier B, Tange S, Tasaki H, Yoshida K, Zhou Y, Sakon N, Katayama K, Nakanishi
589 A.2015. Examination of a plasmid-based reverse genetics system for human astrovirus.
590 *Microbiology and Immunology* 9(10):586-596.
- 591 51. Liu C, Liu WH, Kan LL, Li X, Li YG, Zhao W.2014. Production of polyclonal antibody
592 to a recombinant non-structural protein Nsp1a of human astrovirus. *Journal of Virology Methods*.
593 209:82-85.

594

595

596 **FIGURE LEGENDS**

597

598 **Fig. 1. Construction of nsP1a bait plasmid and detection of**
599 **auto-activation.** (A) Construction of pGBKT7-nsP1a bait plasmid. Lane M:
600 DL15000 DNA marker; Lane 1: amplified fragment of nsP1a; Lane 2:
601 confirmation of pGBKT7-nsP1a by digestion with BamH I and Pst I. (B)
602 Determination of the auto-activation of the pGBKT7-nsP1a bait plasmid in yeast
603 cells. The pGBKT7-nsP1a bait and pGBKT7 plasmids were used to transform
604 Y2HGold cells and then grown on different plates. Co-transformants containing
605 pGADT7-T and pGBKT7-53 were grown on SD -Leu-Trp-His plates as a
606 positive control. Co-transformants containing pGADT7-Lam and pGBKT7-T
607 were grown on SD -Leu-Trp-His plates as negative control. a: pGBKT7-ORF1a
608 + pGADT7; b: pGBKT7-53 + pGADT7-T;c: pGBKT7-Lam + pGADT7-T.

609

610 **Fig. 2. Analysis of putatively positive colonies of Y2HGold cells.** Y2HGold
611 clones containing the cDNA library were grown on dropout medium lacking
612 tryptophan and leucine (SD-Trp-Leu). There were 25 clones, and the total
613 number cloned was 2.5×10^5 . Yeast cells containing the bait (HAstV nsP1a) and
614 prey plasmids (Caco-2 cell cDNA library) were screened for interaction on
615 synthetic dropout media. (A) Screen for interaction on SD-Trp-Leu medium. (B)
616 Screen for interaction on synthetic dropout medium lacking tryptophan,
617 leucine, and histidine (SD-Trp-Leu-His). (C) Screen for interaction on synthetic

618 dropout medium lacking tryptophan, leucine, histidine, and adenine
619 (SD-Trp-Leu-His-Ade). (D) Confirmation of positive interactions on
620 SD-Trp-Leu-X-Gal medium; 15 clones demonstrating protein interactions
621 between HAstV and nsP1a were obtained. Co-transformation with pGADT7-T
622 and pGBKT7-Lam was used as a negative control (-). Co-transformation with
623 pGADT7-T and pGBKT7-53 was used as a positive control (+).
624 Co-transformation with pGBKT7-nsP1a and pGADT7 was used as an
625 auto-activation control (*).

626

627 **Fig. 3. nsP1a interacts with CD63 *in vivo* and *in vitro*.** (A) HEK293T cells
628 were co-transfected with nsP1a-HA plasmid and CD63-Flag plasmid for 48 h
629 and harvested. Cell lysates from co-transfected and untransfected control cells
630 were immunoprecipitated with antibody against Flag or HA and then analyzed by
631 western blot. (B) The recombinant plasmids nsP1a-GST were transfected into *E.*
632 *coli* BL21 (DE3) cells. The cells were then mixed with IPTG at concentrations
633 of 0, 0.1, 0.2, 0.4, 0.8, and 1mM (lanes 1–6, respectively) to induce the
634 expression of nsP1a. The cells were then incubated for an additional 5 h at 25°C.
635 The purified nsP1a-GST protein (110kDa) was analyzed by SDS-PAGE and
636 stained with Coomassie blue R-250 (lane 7). The recombinant protein CD63-His
637 was detected by western blot using CD63 antibody. Lane M: protein molecular
638 weight marker. (C) nsP1a-GST was immobilized on glutathione agarose.
639 CD63-His was then added to assay protein binding. The proteins were washed,

640 eluted from the agarose beads, and confirmed by immunoblotting. The
641 expression of nsP1a was detected by anti-GST mAb. CD63 was detected by
642 anti-His.

643

644 **Fig. 4. The C-terminal nonstructural protein nsP1a/4 interacts with the**
645 **CD63 large loop LEL domain.** Structure of the protein domains of CD63 and
646 the LEL domain. (B) Schematic representation of the protein domains of the
647 HAstV nsP1a protein and the four domains protein tested in this study. (C) The
648 recombinant plasmids CD63-LEL were transfected into *E. coli* BL21 (DE3).
649 The cells were mixed with 0, 0.1, 0.2, 0.4, 0.8, or 1 mM IPTG (lanes 1–6,
650 respectively) to induce CD63 expression, and the culture was incubated for an
651 additional 6 h at 30°C. The purified CD63-LEL-His protein (11 kDa) was
652 analyzed by SDS-PAGE and stained with Coomassie blue R-250 (lane 7). The
653 recombinant protein CD63-LEL was detected by western blot using CD63
654 antibody (lane 8). (D) The recombinant plasmid nsP1a/4-GST was transfected
655 into *E. coli* BL21 (DE3). The cells were mixed with 0, 0.1, 0.2, 0.4, 0.8, or 1 mM
656 IPTG (lanes 1–6, respectively) to induce nsP1a/4 expression, and the culture was
657 incubated for an additional 6 h at 37°C. The purified nsP1a/4-GST protein
658 (66 kDa, GST 26 kDa) was analyzed by SDS-PAGE and stained with Coomassie
659 blue R-250 (lane 7). The recombinant protein nsP1a/4 was detected by western
660 blot using nsP1a/4 antibody (lane 8). Lane M: protein molecular weight marker.
661 (E) nsP1a/4-GST was immobilized on glutathione agarose. CD63-LEL-His was

662 added to assay protein-protein binding. After washing, proteins were eluted from
663 the agarose beads and confirmed by immunoblotting. The expression of nsP1a/4
664 was detected by anti-GST mAb, and CD63-LEL was detected by anti-His. (F)
665 HEK293T cells were co-transfected nsP1a/4-HA plasmid and CD63-LEL-Flag
666 plasmid for 48 h and harvested. Cell lysates from co-transfected and
667 untransfected control cells were immunoprecipitated with antibody against Flag
668 or HA followed by western blot analysis.

669

670 **Fig. 5. Co-localization of nsP1a/4 protein with CD63-LEL protein.** 293 T
671 cells were co-transfected with PEF-nsP1a/4-HA and pcDNA3.1(+)-CD63-LEL
672 Flag plasmids. Cells were fixed after 48 h and subjected to indirect
673 immunofluorescence to detect CD63-LEL-Flag (red, A) and nsP1a/4-HA (green,
674 B) with rabbit anti-Flag and mouse anti-HA antibodies. The position of the
675 nucleus is indicated by DAPI (blue, C) staining in the merged image.
676 Co-expression of CD63-LEL and nsP1a/4 showing cytoplasm localization in
677 merged images D.

678

679 **Fig. 6. CD63 effect on HAstV-1 replication.** The amount of CD63 mRNA
680 expression in the Caco-2 cells infected with HAstV-1 virus by real-time
681 PCR($P < 0.01$); (A) Real time PCR analysis of CD63 mRNA expression in
682 Caco-2 cells infected with HAstV-1. (B) Western blot analysis of CD63 protein
683 expression in Caco-2 cells infected with HAstV-1. (C) Intracellular viral RNA

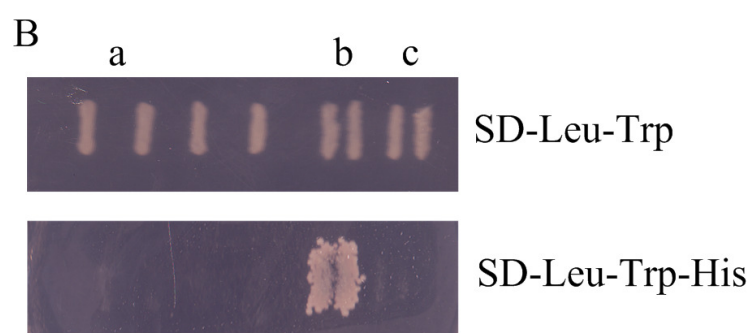
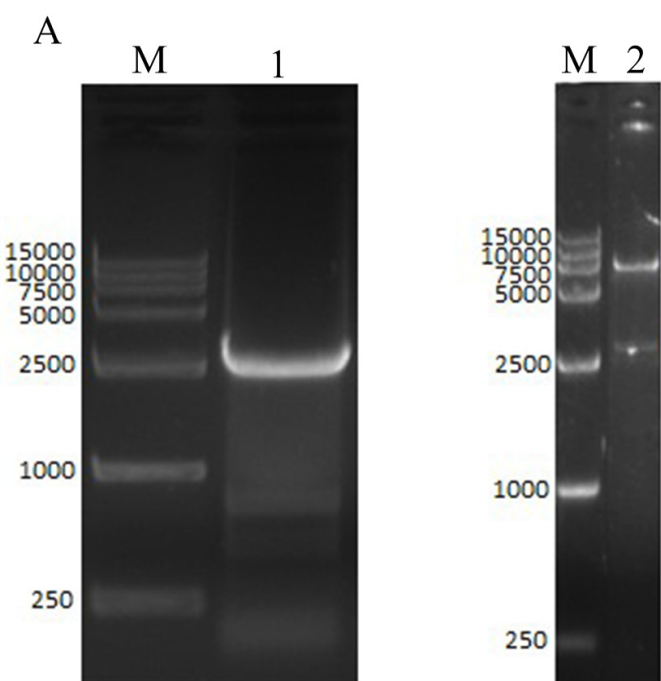
684 levels assayed by real-time PCR ($P < 0.01$). (D) Overexpression of CD63
685 mediated by eukaryotic expression vector pcDNA3.1-3flag and knockdown of
686 CD63 expression mediated by shRNA. (E) Intracellular CD63 mRNA
687 expression levels assayed by real-time PCR ($P < 0.01$). (F) Intracellular viral
688 RNA levels assayed by real-time PCR ($P < 0.01$).

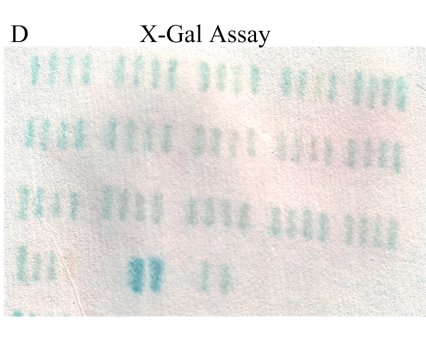
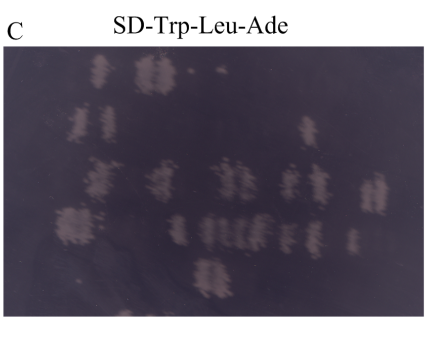
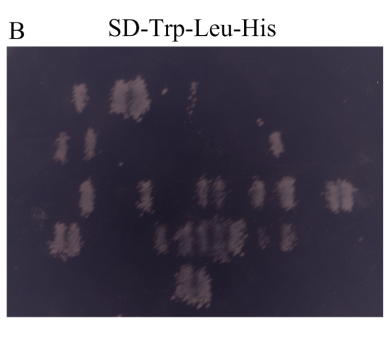
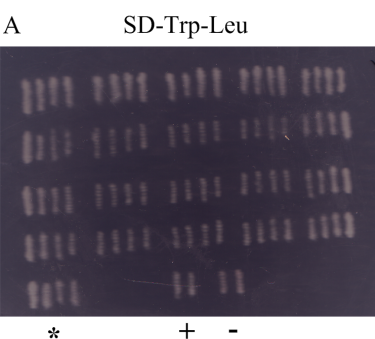
689

690

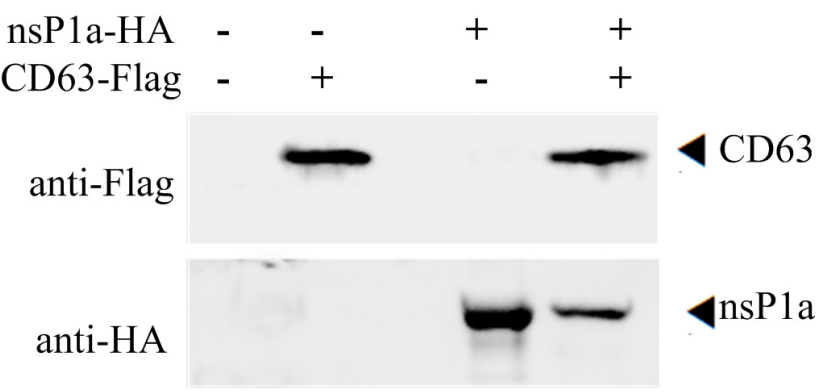
Table 1 Oligonucleotides used in this study

Primer Name	Sequence(5'-3')	Use
Pgex-1a-F	CGC <i>GGATCC</i> ATGGCACACGGTGAGCCATACTATAGT	Construction of pGEX-6P-nsP1a
Pgex-1a-R	CCG <i>CTCGAG</i> ATGAGTGGTAGGTTTGGGCCCTTGG	
Pgex-1a/4-F	CGC <i>GGATCC</i> atg ACCAACACTGGGTATACTGGAGGTG	Construction of pGEX-6P-nsP1a/4
Pgex-1a/4-R	CCG <i>CTCGAG</i> ATGAGTGGTAGGTTTGGGCCCTT	
PET-LEL-F	CCG <i>CTCGAG</i> ATGTATGTGTTTAGAGATAAGGTGA	Construction of pET-29a-LEL
PET-LEL-R	CGC <i>GGATCC</i> CACATTTTCTCAGCCAGCCCCAA	
CD63-GFP-F	CCG <i>CTCGAG</i> GGATGGCGGTGGAAGGAGGAATGAAATG	Construction of pEGFP-N3-CD63
CD63- GFP-R	CGC <i>GGATCC</i> ATCACCTCGTAGCCACTTCTGATA	
CD63-3flag- F	CCC <i>AAGCTT GCCACC</i> ATGGCGGTGGAAGGAGGAATGAAATG	pcDNA3.1-3flag-CD63
CD63-3flag- R	CCGCTCGAGTTACTTATCGTCGTCATCCTTGTAATCCATCACC TCGTAGCCACTTCTGATAC	
LEL-3flag- F	CCC <i>AAGCTT GCCACC</i> ATGTATGTGTTTAGAGATAAGGTGA	pcDNA3.1-3flag-CD63-LEL
LEL-3flag -R	CCGCTCGAGTTACTTATCGTCGTCATCCTTGTAATC CACATTTTCTCAGCCAGCCCCAA	
1a-HA-F	Gactagcc ATGGCACACGGTGAGCCATACTA	PEF-HA-PGK-hygro-1a
1a-HA-R	TTCGTCGACATCGATGGATCC ATGAGTGGTAGGTTTGGGCCCTT	
1a/4-HA-F	gactagcc ATGACCAACTGGGTATACTGGAG	PEF-HA-PGK-hygro-1a/4
1a/4-HA-R	TTCGTCGACATCGATGGATCC ATGAGTGGTAGGTTTGGGCCCTT	
CD63-shRNA-1-F	GATCCCgcAAGGAGAACTATTGTCTTACTCGAGTTTTGGAT TAAGACAATAGTTCTCCTTGC	hU6-shRNA- CD63-1
CD63-shRNA-1-R	AGCTATCCAAAAgcAAGGAGAACTATTGTCTTACTCGAG TAAGACAATAGTTCTCCTTGC	
CD63-shRNA-2-F	GATCCCgcTGGCTATGTGTTTAGAGATCTCGAG ATCTCTAAACACATAGCCAGC TTTTGGAT	hU6-shRNA- CD63-2
CD63-shRNA-2-R	AGCTATCCAAAAgcTGGCTATGTGTTTAGAGAT CTCTCGAG ATCTCTAAACACATAGCCAGCGG	
CD63- QPCR-F	GTGGAAGGAGGAATGAAATGTGT	CD63 mRNA quantity
CD63- QPCR-R	AAAGCCACCAGGAAGAGGAAG	SYBR method for Real time PCR
HAstV-QPCR-F	AAATCAAGAGCCCGTTCA	Viral mRNA quantity (ORF2 gene)
HAstV-QPCR-R	ACGCCTCAATCTCGGTAG	SYBR method for Real time PCR

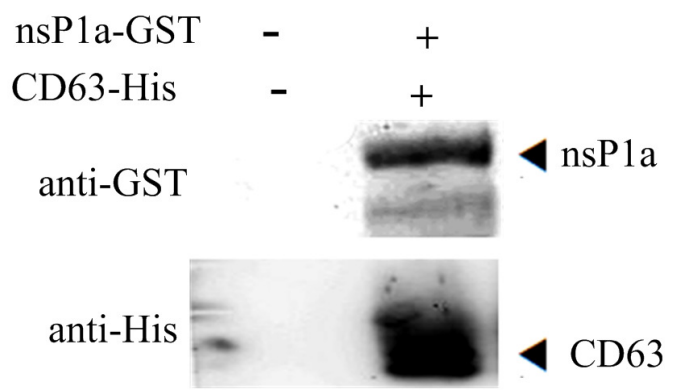




A



C



B

